Fatigue of Welded Steel Structures due to Strong Earthquakes

—Strain Controlled Low-Cycle Fatigue Tests of Cylindrical Specimens—

By

Kiyoshi KANETA and Isao KOHZU

(Received September 30, 1980)

Abstract

This experiment was carried out in order to examine cyclic inelastic actions and low-cycle fatigue properties of butt welded joints of steel structures. Base metals which consisted of mild to high tensile strength steel, namely, SS41 to HT80, were used. The welded joints were made by means of various kinds of butt welding processes. These base metals and the welded joints were fabricated and shaped into cylindrical specimens, and loaded cyclically by an uniaxial tension-compression method, to the point where the specimens were fractured.

No significant differences between the base metal and the welded joint were observed with respect to the cyclic stress-strain relationships and the energy absorption capacities at the steady-state in non-dimensional forms. However, as for fatigue strength, some deterioration was observed at the lower cycles with regard to the welded joints of the base metals whose monotonic tensile strength is relatively high.

New quantitative estimations with respect to energy absorption capacity and low-cycle fatigue strength deterioration are also proposed herein.

1. Introduction

When a steel structure is subjected to destructive earthquakes, low-cycle fatigue damage of the members or sub-assemblages may possibly occur due to repeated elasto-plastic deformations. The possibility that low-cycle fatigue damage may occur in any particular structural component depends mainly upon a) the strength, ductility and the energy absorption capacity of the components, and b) the intensity and duration of the earthquake to which the structure would be subjected.

In order to gauge the effects of the former group of factors on low-cycle fatigue damage, experimental research is required to confirm cyclic inelastic deformation characteristics and low-cycle fatigue properties of structural steels, members and subassemblages. Attempts to clarify low-cycle fatigue properties of several struc-

Department of Architectural Engineering

tural steels, metals and alloys have been developed by past investigators: Manson[1] and Coffin[2] proposed the well-known Manson-Coffin formula to express low-cycle fatigue lives, and elastic and plastic strain amplitudes. Yao and Munse[3] proposed a "low-cycle fatigue-damage" model based upon a hypothesis which limited the effect to plastic true strains in tension sides. Morrow[4] and Feltner[5] investigated the characteristics of the cyclic plastic strain energy and low-cycle fatigue. In later years, modified Manson-Coffin formulae were reported by several investigators[6-12], by which other experimental formulae[13-16] were found to give accurate estimates of low-cycle fatigue lives of metals.

On the basis of these quantitative estimations, it has been possible for investigators to numerically compute low-cycle fatigue damage of steel structures subjected to destructive earthquake motions. Kajiraj and Yao[17] calculated fatigue damage factors which single degree of freedom structures with various structural properties (i.e., natural periods, strength parameters and damping coefficients, etc.) would suffer as a result of two strong earthquake motions. Another investigation was carried out by Kajiraj[18] to determine the low-cycle fatigue damage in multistory structures. In the analysis, it was pointed out that the aseismic safety of structures is not necessarily related directly to the maximum deflection ratio. Hence, as a guideline to the safety of structures, it may be necessary to figure out the values of the fatigue damage factor in structures which may undergo inelastic deformations in the event of earthquakes.

Suidan and Eubanks[19] investigated the cumulative low-cycle fatigue damage of single degree of freedom steel frames by proposing another damage model. In the investigation, the rain flow cycle counting method was employed in order to evaluate the cumulative fatigue damage.

Mizuhata et al.[20] evaluated the relationship between plastic story to story displacements and fatigue lives from the results of the experiments conducted on single story and one bay steel frames and steel-concrete frames subjected to constant distortion amplitudes and dynamic excitations, that is, white noise. From these experimental results, a low-cycle fatigue damage was calculated for low to high rise steel frames subjected to a strong motion, using several damage counting methods.

In the aforementioned investigations, it has been proposed that columns in particular would suffer severe damage from exposure to strong earthquake motions. However, some consideration should be given to the possibility of incremental collapse due to the so-called P-Δ effect which is ignored except in a certain report[20]. Generally, in designing steel structures against severe earthquake damage, it is necessary to allow for the generation or occurrence of inelastic deformations

in the structural components. In these cases, as Anderson and Gupta[21] suggested, it may be desirable that these inelastic deformations should be generally confined to the girders because of safety considerations, ease of repair and the fact that they will remain functional.

Consequently, it is desirable to design steel structures as a weak-beam, strong-column type. This would confine the strains to the elastic range of the column sections during earthquake excitations. In this case, there is a great deal of interest in regard to its behaviors, in terms of inelastic cyclic action, dissipation of energy and low-cycle fatigue of the girders. We must especially pay much attention to the actual behavior of girder ends, and to points near or at connections. These locations could possibly become the most critical sections under the influence of bending and shear stresses which occur when dead and live loads set along the girders are compounded with the lateral load imposed upon the frames during earthquakes.

In the event that the girders comprise wide flange sections, it often happens that the girder flanges are butt welded to column flanges and the girder webs bolted with gusset plates welded to the column flanges (or fillet or butt welded to them). Thus, it is reasonable to assume that the cyclic load carrying capacity and the inelastic deformation capacity located at girder ends may be inferior to those at the original wide flange section. This would be due to a reduction in the cross sectional area caused by scalloping which is done to insure the welding performance, and also by the occurrence of tempering and residual stresses as a result of welding.

For the above reasons, it is important to clarify the actual inelastic behaviors at girder ends experimentally and analytically.

An earlier investigation by Tanabashi[22] reported on tests used to determine the behavior of the welded joints of steel members under alternating bending. Many investigators have since studied the behavior of beams, beam-column connections and frames under alternating bending moments and lateral loadings.

Popov and Bertero[23] tested cantilever beam connections actually used in the construction of high rise steel buildings in order to determine the cyclic behavior and energy absorption capacity. The normalized curvature capacity of the connections which were determined in these experiments provided guidelines for the analysis and design.

However, many investigations, with few exceptions[20,22,23], virtually leave untouched the question of whether or not any deterioration of deformation capacity, energy absorption capacity and fatigue strength of those structural components occurs with respect to the welded girder ends subjected to alternating

plastic bending, especially, in relation to the precise comparison between base metal and the welded joint.

In the present experiment, the authors have employed cylindrical specimens to investigate whether or not welded joints undergo any deterioration in comparison with base metals, from mild steel to high tensile strength steel. In this paper, a method of quantitative estimation has been developed to verify cyclic inelastic action and fatigue strength for welded joints.

2. Experimental Procedures

2.1 Objectives

Generally speaking, as a first order approximation, the upper or the lower girder flange of the wide flange section of an actual steel girder may be considered as being subjected to the tension or compression axial force. This especially pertains to the actual beam-column welded connection which has a reduced cross sectional area caused by scalloping. The use of round bars serve to eliminate the differences due to geometrical shape or stress distributions from the actual welded joint. As a result, fatigue tests under uniaxial loadings which use the round bars fabricated from welded plates provide a simple and fundamentally efficient means for arriving at a general estimate of cyclic inelastic deformation characteristics and low-cycle fatigue properties of the actual beam-column welded joints. Few past investigations[24-27] which adequately deal with these aspects, however, have been conducted, especially, with respect to ultra low-cycle fatigue phenomena which occur in the range of up to several hundreds of cycles. Thus, the first experiment was conducted to clarify the aforementioned problem by using various specimens comprising several kinds of base metals, from mild to high tensile strength steel, as well as welded joints under uniaxial loadings.

2.2 Review of Experiment

2.2.1 Varieties of Structural Steel Plates and Welding Processes

The varieties of the structural steels used in this investigation were SS41, SM50B, SM58Q, HT70 and HT80 of 25 or 32 mm thick steel plates, with a portion of HT80 consisting of 75 mm thick plates. The mechanical properties and chemical compositions for these kinds of steel plates are listed in Table 1.

The connections were welded at right angles to the rolled section of each plate along the weld line. The welding process used for each steel plate is given in Table 2. Almost all grooves were squares, with the exception of HT70, in which an X-shaped double groove butt weld was selected because of the difficulty of electroslag square butt welding. All the welded joints were inspected for weld

Table 1. Material Properties

		SS41	SM50B	SM58Q	HT70	HT80*	HT80
Mechanical Properties	Yield Point (kg/mm²)	28	41	64	66	78	85
	Tensile Strength (kg/mm²)	44	58	75	72	84	89
	Elongation (%)	25	24	42	28	24	26
	Impact Test (kg·m)		5.7	24.3	17.5	17.3	17.9
Chemical Composition (%)	C	0.24	0.18	0.16	0.09	0.12	0.11
	Si	0.02	0.42	0.34	0.28	0.36	0.26
	Mn	0.99	1.37	1.37	0.80	0.98	0.91
	P	0.016	0.04	0.012	0.014	0.006	0.011
	S	0.02	0.02	0.004	0.011	0.004	0.009
	Cu				0.02	0.50	0.26
	Cr				0.40	0.23	0.44
	Ni				1.24	1.27	0.51
	Mo				0.43	0.51	0.50
	V				0.03	0.03	0.038
	Ceq	0.41(1)	0.43(1)	0.31(2)	0.45(1)	0.57(1)	0.50(1)

* plate thickness=75 mm
(1) Ceq=C+Mn/6+Si/24+Ni/40+Cr/5+Mo/4
(2) Ceq=C+Mn/9+Ni/40+Cr/20+Mo/8+V/10

defects by means of an X-ray radiographic inspection to insure no serious defects were contained.

Table 2. Welding Processes

SS41	Electroslag
SM50B	"
SM58Q	"
HT70	CO_2 Arc or Submerged Arc
HT80	Mig (Shield Gas: Ar (80 %)+ CO_2 (20%))

2.2.2 Specimens

Fig. 1 shows the shape and the size of the test specimens fabricated from the original plates and the welded joints. For a part of SS41, the gauge length was determined at the range of 10 mm. The specimens were classified into base metals, weld metals, and heat-affected zones, with the exception of the HT70 specimens. In the case of HT70, the groove shape made the assortment of weld metal and heat-affected zones difficult, and so the specimens composed of base metal and weld metal were used.

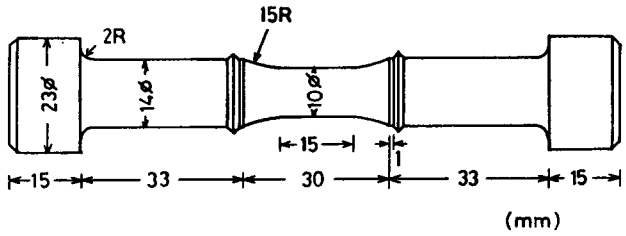

Fig. 1. Specimen

These classifications of welded joints were made by inspecting whether or not the ranges of weld metals or heat-affected zones were within the parallel portion of the bar in Fig. 1, and the positions were fixed near or at the specimen's center. This was done only after the surface corrosion test using a solution of nitric acid.

2.2.3 Experimental Procedure

Cyclic tests and monotonic tension tests were carried out. The former tests were conducted under constant distortion (or strain) amplitudes at longitudinal points along the specimens. Distortion (or strain) amplitudes were detected by a pair of electric extensometers connected to the specimens at the projections, as shown in Fig. 1. As is evident from the figure, the distortion amplitudes of the gauge lengths are somewhat different from those between the projections. For this reason, the plastic strain gauges were pasted within the gauge lengths and the outputs were compared with those of the extensometers. The calibration curves were in this way recorded and were later used in connection with the cyclic tests. But, as some degree of drift had been observed on the strain measurements of plastic gauges after repeated loadings, new plastic strain gauges were pasted on after steady states, and it was confirmed that no significant differences had occurred in the detection of strain measurement between the initial-state and the steady-state.

An electronic universal testing machine (AUTOGRAPH) with a 10 ton capacity was used to load, and the load-deflection curves were automatically recorded on an X-Y recorder. The selected strain amplitudes for all specimens were in the range of $\pm 0.5\%$ to $\pm 4.0\%$ in cyclic tests, and the work was terminated after the specimens were perfectly fractured on the tension sides. The cross-head speed of AUTOGRAPH was maintained at a constant rate between 0.5 to 5.0 mm/min.

3. Results and Experimental Considerations

3.1 Monotonic Tension Tests

Monotonic tension tests on five kinds of base metals, weld metals and the heat-affected zones were carried out. No significant deterioration of the welded joints in comparison with the base metals was observed. As far as the monotonic tension tests are concerned, the good ductility comparing with the base metals has been explained as the reason. These results are shown in Table 3.

3.2 Stress-Strain Relationships at Steady-States under Cyclic Loading

As other investigators[4,12] have pointed out, the following descriptions may

Table 3. Results of Monotonic Tensile Tests

	SS41			SM50B			SM58Q			HT70			HT80		
	B.	W.	H.	B.	W.	H.	B.	W.	H.	B.	SW.	C.W.	B.*	W.	H.
σ_u	43.5	51.0	45.5	54.8	59.1	57.7	75.7	72.6	73.7	76.1	76.1	72.8	88.3	88.5	76.7
ε_f	1.04	0.98	0.84	1.24	1.06	0.76	1.20	1.04	0.97	1.18	0.94	1.03	1.02	1.26	1.26

B. : Base metal, W. : Weld metal (SW. : Weld metal of Submerged Arc W. and C.W. : Weld metal of CO_2 W. for HT70) and H. : Heat affected zone
* : plate thickness=75 mm
σ_u : the nominal tensile strength (kg/mm²)
ε_f : static fracture ductility

be given as to the sequence followed from the initial-state to the final one; namely, specimens of SS41 base metal and the welded joints show that a cyclic softening occurs within $\pm 0.5\%$ strain amplitude; that a cyclic hardening occurs after several cyclic loadings at the steady-state beyond this amplitude; and that constant stress amplitudes are maintained throughout the overall cycles.

In the cases of the SM50B and SM58Q specimens, hardening was observed at the first 2 cycles followed by a very slight softening which occurred in almost all selected strain amplitudes. The specimens then arrived at a steady-state which was approximately 20% of the cycles at which the specimens were fractured.

However, in the cases of the HT70 and HT80 specimens, after cyclic hardening occurred at 2 cycles, a slight decrease of stress amplitudes was maintained, and distinct steady-states were not observed. Moreover, after an abrupt fall of stress amplitudes occurred at 80% of cycles to failure, the specimens were brittle fractured.

Typical examples for the SM50B and HT80 specimens are shown in Fig. 2.

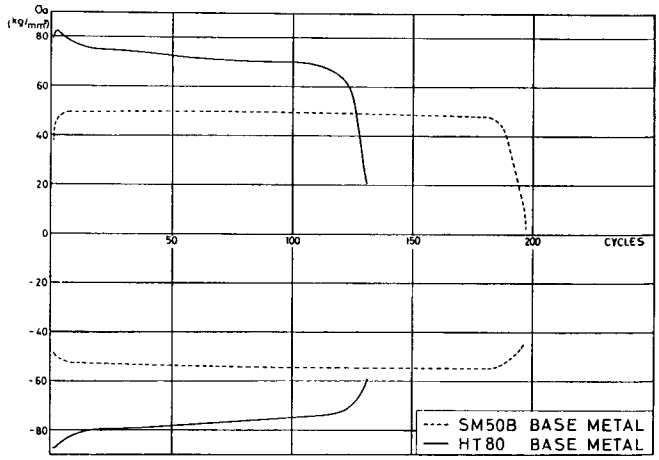

Fig. 2. Typical Examples of Peak Stresses-cycles Relations

As mentioned above, it may be difficult to define the steady-states distinctively for all specimens. Also, in this investigation, it has been considered that the number of cycles at the steady-states were about 20% of lives.

Cyclic stress-strain relationships have been investigated by many investigators. In this paper, the authors adopted the method proposed by Morrow[4], with notations of cyclic stress-strain curves at the steady-states shown in Fig. 3.

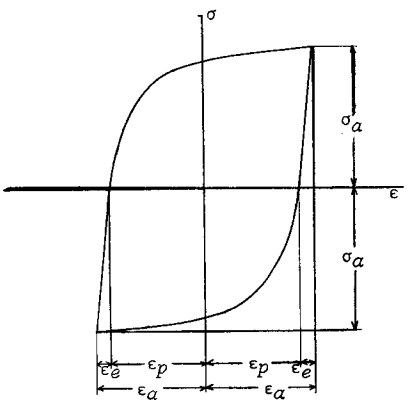

Nomenclature

σ_a	Stress amplitude
ε_a	Strain amplitude
ε_e	Elastic strain amplitude
ε_p	Plastic strain amplitude

Fig. 3. Nomenclatures of Stress-strain Curves at the Steady-states

Non-dimensional forms which are arrived at by dividing the stress and strain amplitudes by the yield stresses and strains (or 0.2% off-set ones) were used in testing several strength steels and the welded joints. Log-log plots of the data for each base metal and the welded joints are presented in Fig. 4 (a)-(e). From these figures, it may be possible to conclude that the non-dimensional stress-strain relationship of the welded joint, at the steady-state, is not different from that of the base metal. In Fig. 4 (a)-(e), after applying the least squares method, the following approximation formula was derived:

$$\sigma_a/\sigma_y = A \cdot (\varepsilon_p/\varepsilon_y)^B \qquad (1)$$

where σ_y: the yield stress

ε_y: the yield strain (or 0.2% off-set strain)

Table 4. Coefficients and Constants of Eq. 1

	A	B
SS41	0.89	0.22
SM50B	0.84	0.17
SM58Q	0.85	0.15
HT70	0.91	0.12
HT80	0.90	0.10

The constant A and the coefficient B of Eq. (1) are tabulated in Table 4. As is apparent from this table, it can be considered that the constant A is not sensitive to base metal strength, but that the coefficient B is significantly influenced and decreases as the base metal strength increases. Thus, a log-log plot between the average of nominal tensile strength of base metal and the welded joint, and the coefficient B was performed, with the result shown in Fig. 5. From this figure, the coefficient B can be well represented by the following function for the nominal tensile strength.

Namely,

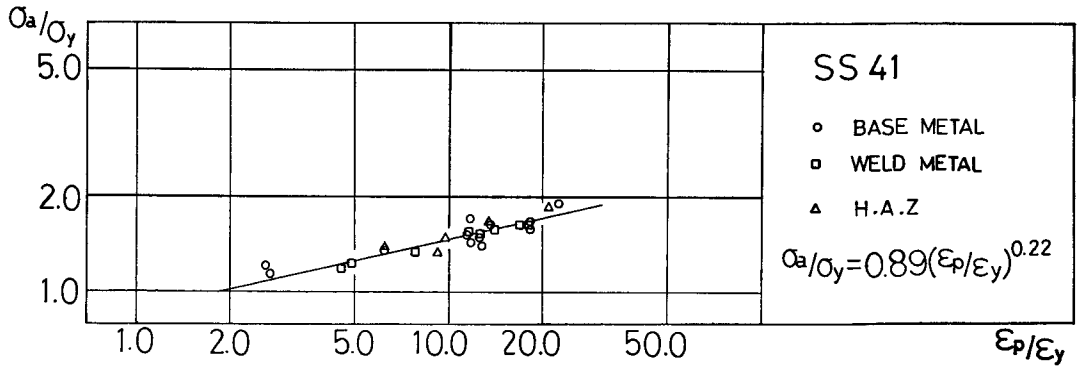
σa/σy
5.0
2.0
1.0
1.0
2.0
5.0
10.0
20.0
50.0
εp/εy
SS 41
BASE METAL
WELD METAL
H.A.Z
σa/σy=0.89(εp/εy)^0.22

(a)

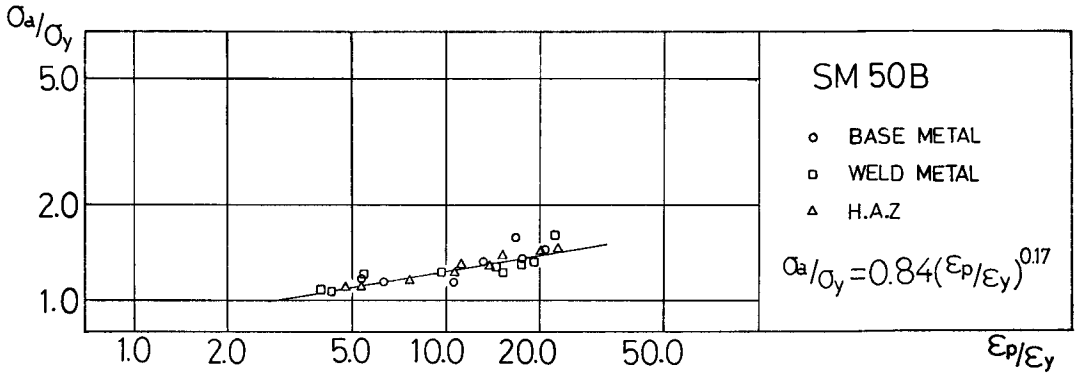
σa/σy
5.0
2.0
1.0
1.0
2.0
5.0
10.0
20.0
50.0
εp/εy
SM 50B
BASE METAL
WELD METAL
H.A.Z
σa/σy=0.84(εp/εy)^0.17

(b)

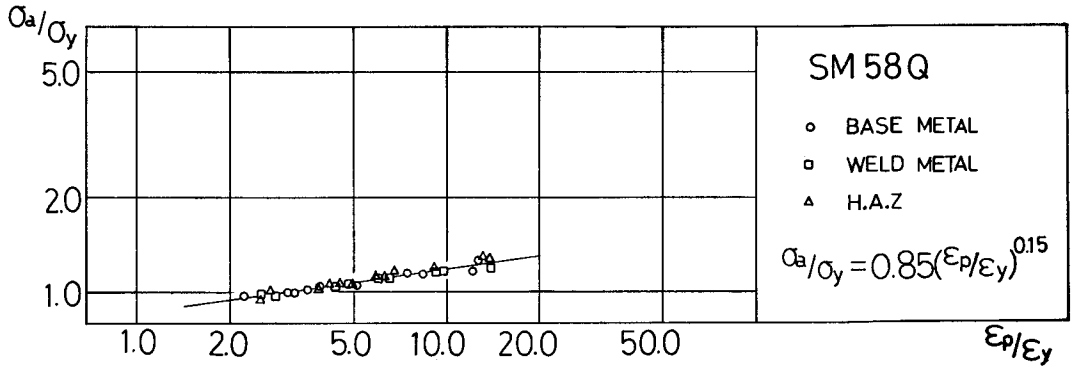
σa/σy
5.0
2.0
1.0
1.0
2.0
5.0
10.0
20.0
50.0
εp/εy
SM 58Q
BASE METAL
WELD METAL
H.A.Z
σa/σy=0.85(εp/εy)^0.15

(c)

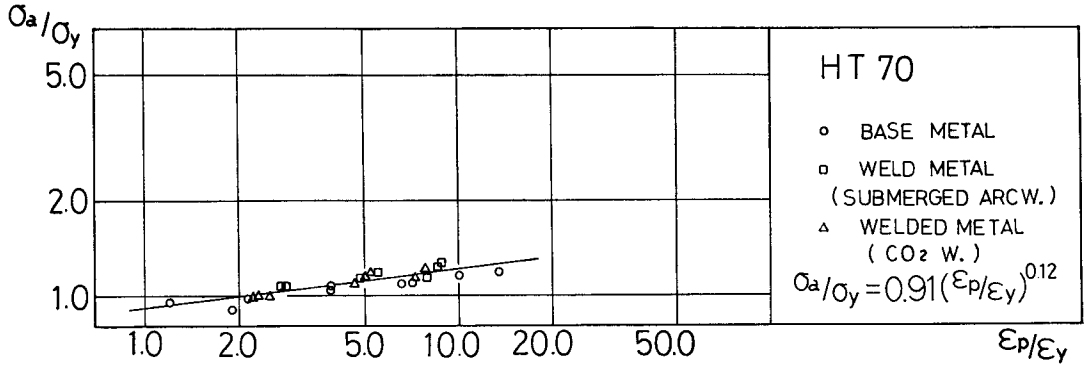

(d)

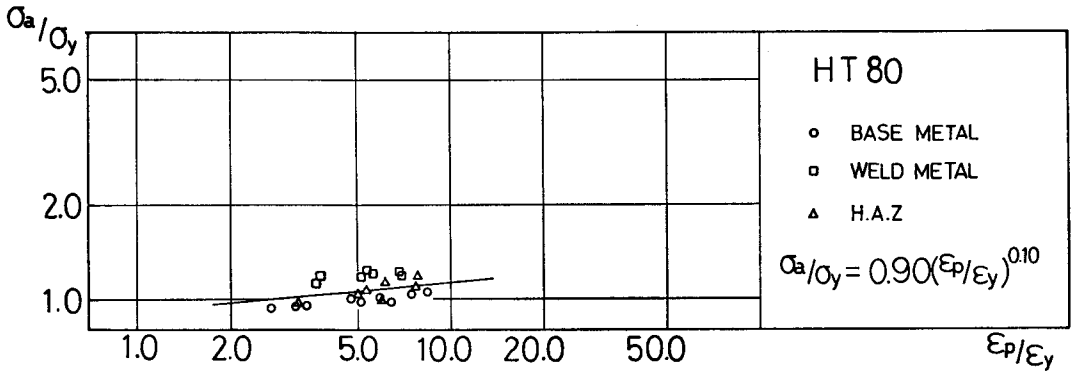

(e)

Fig. 4. Non-dimensional Cyclic Stress-strain Relations at the Steady-states

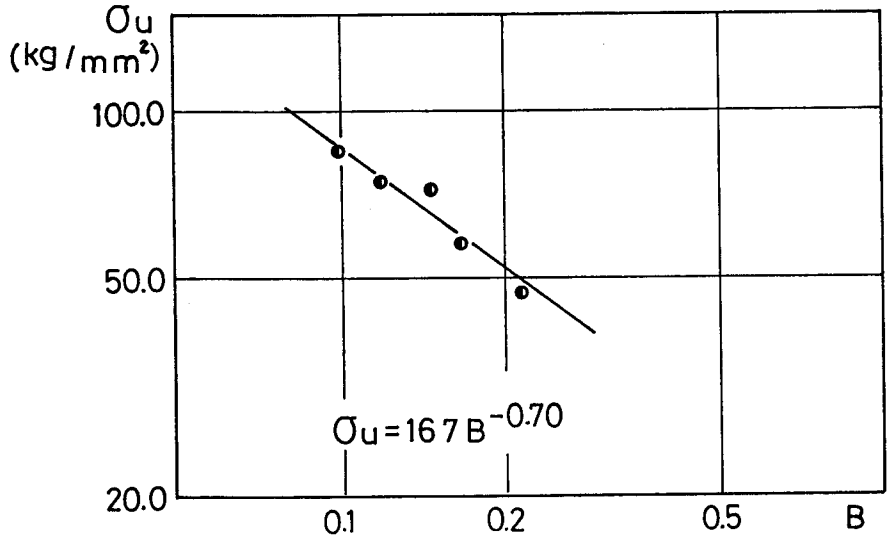

Fig. 5. The Nominal Tensile Strengths and the Coefficients B Relations

$$\sigma_u = 16.7 \cdot B^{-0.70} \qquad (2)$$

where σ_u: the nominal tensile strength

3.3 Relation between Plastic Strain Energy per Cycle and Plastic Strain Amplitude

In order to assess the aseismic safety of steel structures in the event of destructive earthquakes, it is crucial to understand the quantitative mechanics of energy absorption on the frames or the sub-assemblages, as the presupposition of consideration upon the low-cycle fatigue damage. Toward the end, a method was proposed for approximating a quantitative expression per cycle of plastic energy, that is, the non-dimensional plastic energy per cycle at selected strain amplitudes divided by the absorbing energy capacity at the elastic limit in the initial-state was related to the cyclic plastic strain amplitude in the non-dimensional form.

Log-log plots for all types of specimens are represented in Fig. 6 (a)-(e). From these figures, as there is no significant difference of the absorbing energy amount with respect to each base metal and the welded joint, each linear approximation on a log-log scale can be formulated as follows;

$$\bar{e} = C \cdot (\varepsilon_p/\varepsilon_y)^D \qquad (3)$$

where $\bar{e}$: non-dimensional plastic energy per cycle, namely, which are obtained by dividing W (the plastic strain energy per cycle) by $\sigma_y \varepsilon_y/2$,
C: the constant, and
D: the coefficient.

Table 5. Coefficients and Constants of Eq. 3

	C	D
SS41	5.71	1.24
SM50B	5.10	1.20
SM58Q	5.30	1.19
HT70	5.62	1.18
HT80	5.63	1.19

The calculated values of C and D for the specimens used are summarized in Table 5.

4. Fatigue Strength of Welded Joints

4.1 Survey and Discussion

Several experiments have been carried out by other investigators with respect to low-cycle fatigue strength, as mentioned in the previous section. However, a method for accurately expressing low-cycle fatigue strength needs to be formulated. Herein, the well known Manson-Coffin formula is regarded as being unsatisfactory. Since a linear relationship would not apply to all kinds of metals, the Manson-Coffin formula tends to be deficient, in that it does not consider the differences in materials, specimen shape, experimental velocities, laboratory condition, etc.

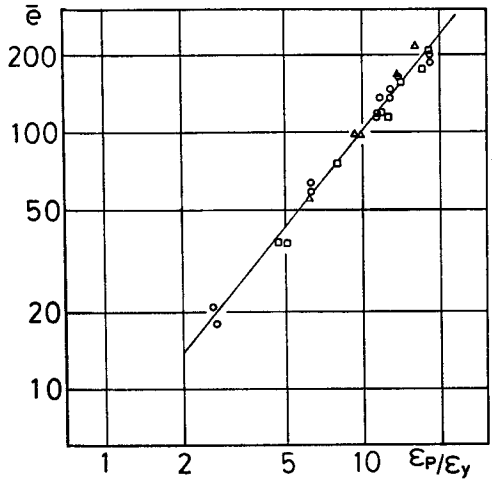
ē
200
100
50
20
10
1
2
5
10
εp/εy
SS 41
BASE METAL
WELD METAL
H.A.Z.
ē=5.71(εp/εy)^1.24

(a)

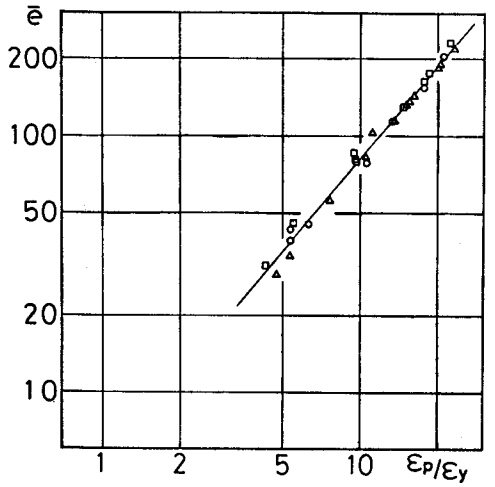
ē
200
100
50
20
10
1
2
5
10
εp/εy
SM 50B
BASE METAL
WELD METAL
H.A.Z.
ē=5.10(εp/εy)^1.20

(b)

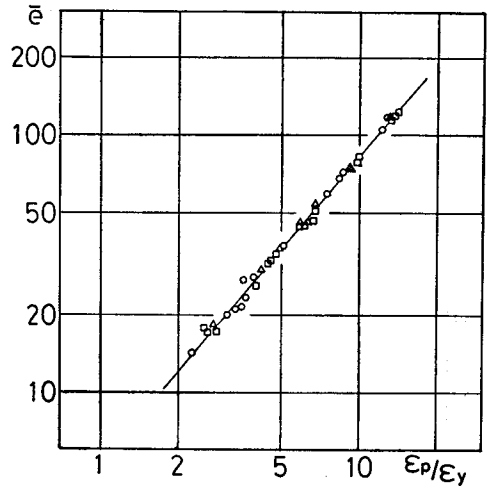
ē
200
100
50
20
10
1
2
5
10
εp/εy
SM 58Q
BASE METAL
WELD METAL
H.A.Z.
ē=5.30(εp/εy)^1.19

(c)

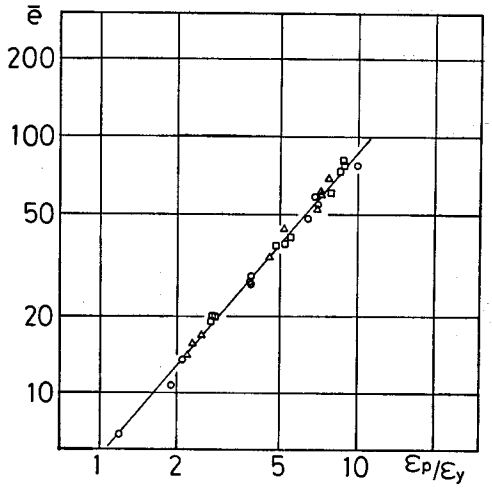
ē
200
100
50
20
10
1
2
5
10
εp/εy
HT 70
BASE METAL
WELD METAL
(SUBMERGED ARC W.)
WELD METAL
(CO2 ARC W.)
ē=5.62(εp/εy)^1.18

(d)

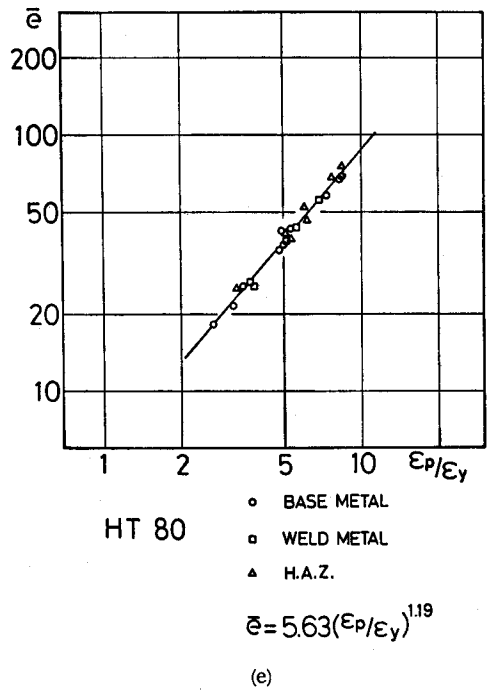

(e)

Fig. 6. The Non-dimensional Plastic Strain Energy per Cycle and the Plastic Strain Ductility Relations

For example, Hotta et al.[7-9] reported that the fatigue strength predictions arrived at by Manson-Coffin formula are in many cases dubious. Further, divergences from Manson-Coffin linear relationship exist and kink points were observed in the relationship between ε_p and N_f (fatigue life) on a log-log scale, for the metals which possess strength levels above about 60 kg/mm^2. For this reason, Hotta et al.[7-9] proposed an empirical but modified formula for the metals without any kink phenomena, and another formula, using the total strain amplitude and fatigue life to failure for the metals which exhibit the kink phenomena.

Moreover, Yagi et al.[14-16], taking into consideration the fact that the damage which is basically dependent upon static fracture ductilities, is different in the first and final cycles from that in other cycles, proposed that damages, except those which are in the initial and final cycles, can be predicted by the power functions which are determined by the use of plastic strain amplitudes and cyclic stress-strain relations.

The authors have already reported elsewhere[28] that neither the Manson-Coffin formula nor the proposed method which involves determining the coeffici-

ents of the formula, would be adequate for the welded joints. This conclusion was based upon experimental results, some of which are included in this experiment.

Secondly, few investigations concerning low-cycle fatigue properties of welded joints have been conducted as compared with the numerous investigations on different types of base metals. For instance, Iida[24] suggested that the fatigue deterioration due to welding can be shown by the fatigue strength ratio to the crack initiation life, and that the fatigue strength of the welded joints is inferior to those of the base metal within the lower range of about 5×10^3 cycles. This was in an experiment carried out using A302B steel and welded joints under uniaxial loadings with selected constant strain amplitudes.

It is reasonable to consider that no physical meaning exists between the plastic strain amplitude and the fatigue life in the linear relation of the Manson-Coffin formula, as has been reported by Yagi et al.[14-16]. The authors of the present paper, however, stand on the viewpoint that when the data is empirical, the Manson-Coffin formula could be fundamentally applied to advantage, although the coefficients themselves would have to be inherent values dependent upon the material properties, specimen shapes, etc., as are practical to engineering demands.

From the above discussion, the objectives in this section are to try to formulate a method for making fatigue strength predictions for welded joints, and to quantitatively clarify the nature of fatigue deterioration of welded joints compared with the base metals. Special features in this paper exist in the following aspects, namely, the non-dimensional plastic strain amplitude $\varepsilon_p/\varepsilon_y$ and the following defined fatigue life N_f' should be used instead of the plastic strain amplitude ε_p and the number of cycles to failure N_f, respectively. The former is based upon the finding that the experimental results show scattered signs of strain at the yield points (or 0.2% off-set strain). Even if the selected strain amplitude was the same for specimens of the same lot, this would further cause the pattern distribution of fatigue lives to become dispersed. It can be concluded that the initial yield strains (or 0.2% off-set strains) are inherent because of the considerable differences with respect to surface finishings and residual stresses, mainly caused by welding. These influences cannot be neglected, especially, in the case of the welded joints.

Another proposal is to adopt the value N_f' which is obtained by dividing the total dissipated plastic strain energy to failure by the plastic strain energy per cycle at the steady-state. The reason for this is that random crack formation and propagation would tend to disperse the experimental results for the number of

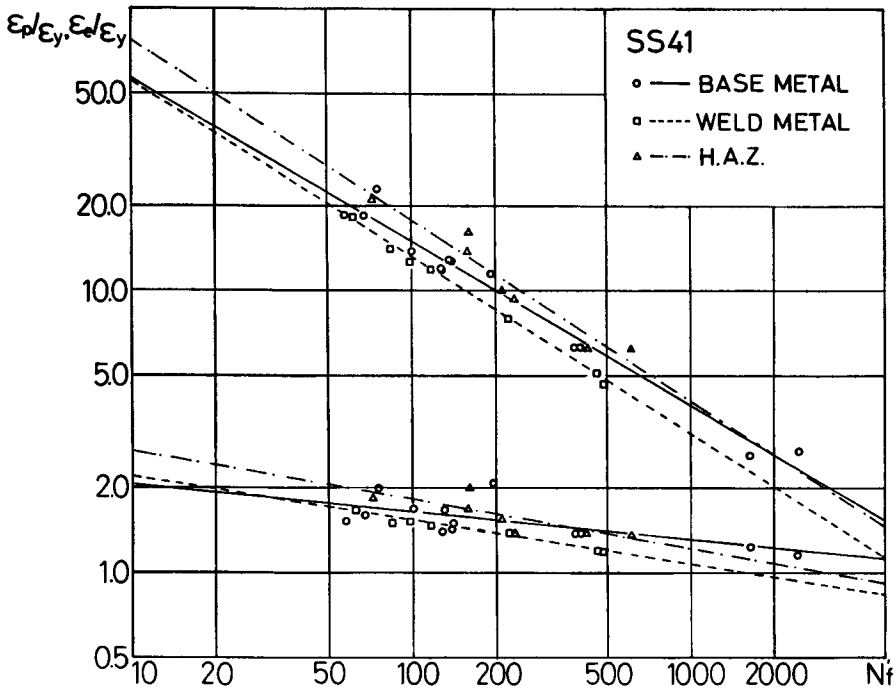
εp/εy, εe/εy
SS41
BASE METAL
WELD METAL
H.A.Z.
50.0
20.0
10.0
5.0
2.0
1.0
0.5
10
20
50
100
200
500
1000
2000
Nf

(a)

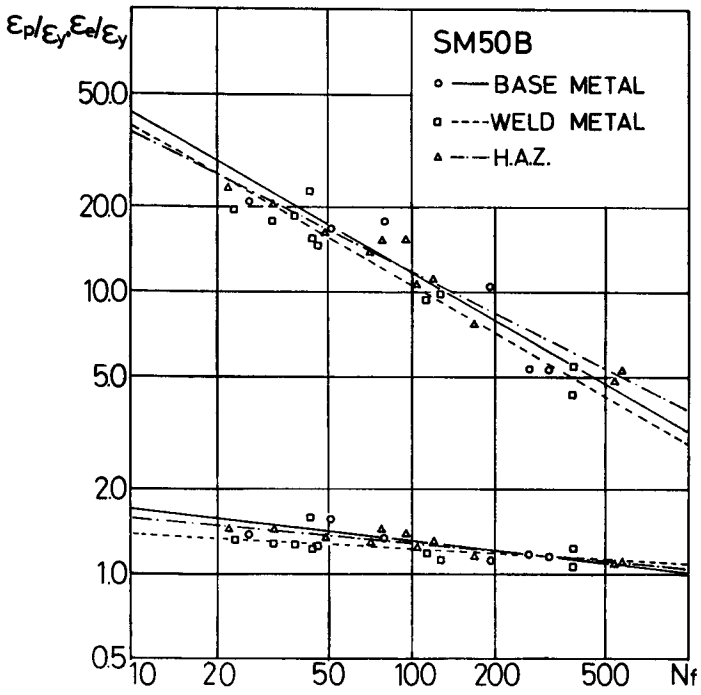
εp/εy, εe/εy
SM50B
BASE METAL
WELD METAL
H.A.Z.
50.0
20.0
10.0
5.0
2.0
1.0
0.5
10
20
50
100
200
500
Nf

(b)

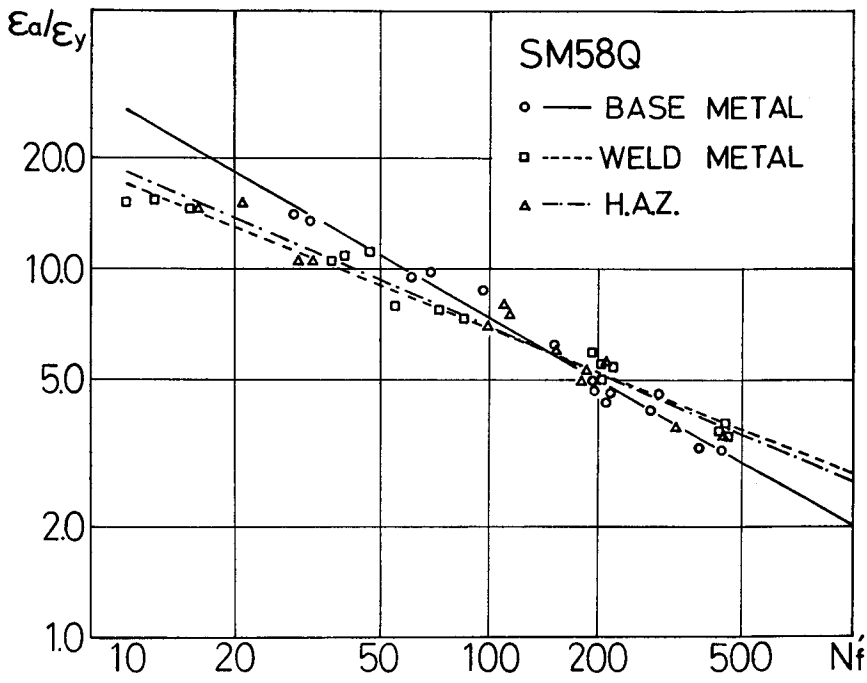
εa/εy
SM58Q
BASE METAL
WELD METAL
H.A.Z.
20.0
10.0
5.0
2.0
1.0
10
20
50
100
200
500
Nf

(c)

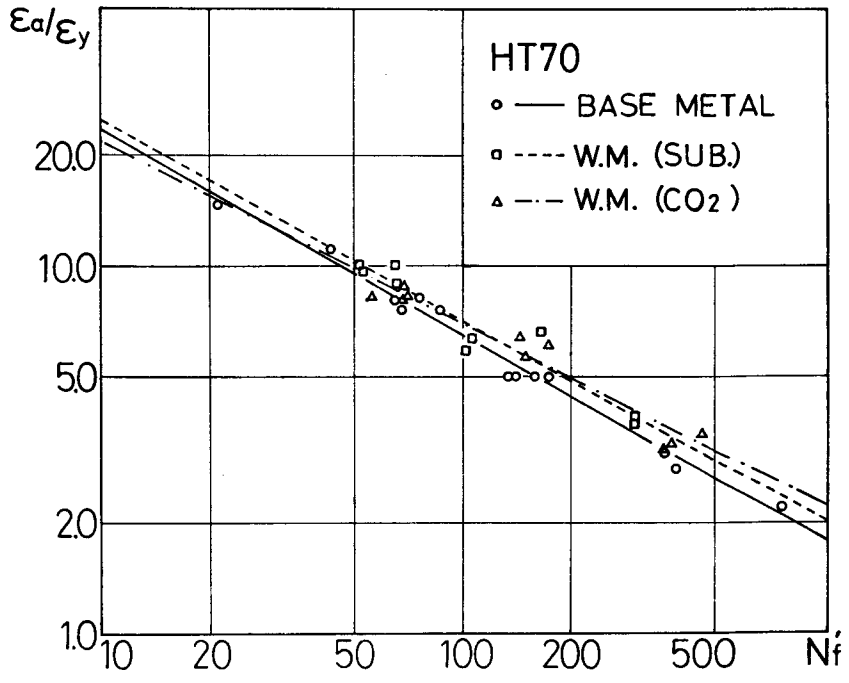
εa/εy
HT70
BASE METAL
W.M. (SUB.)
W.M. (CO2)
20.0
10.0
5.0
2.0
1.0
10
20
50
100
200
500
Nf

(d)

cycles to failure N_f carried out under the same selected strain amplitudes.

For overall results that were arrived at by such methods, the following predictions of fatigue lives were conducted.

4.2 Estimates of Low-Cycle Fatigue Strength and Fatigue Deterioration of Welded Joints

According to Hotta method[7-9], it was assumed that the following two types of linear approximations could be applied satisfactorily. For the metals below SM50B, the Manson-Coffin linear relations could be applied to experimental results, which entail dividing the total strain amplitudes into plastic and elastic strain amplitudes in the non-dimensional forms. For results on the metals above SM58Q, another linear relation, between non-dimensional total strain amplitudes and fatigue lives, was applied.

These non-dimensional strain amplitudes and correspondent fatigue lives calculated from the dissipated plastic strain energy were plotted on a log-log scale. The results are shown in Fig. 7 (a)-(e), with respect to base metals and welded

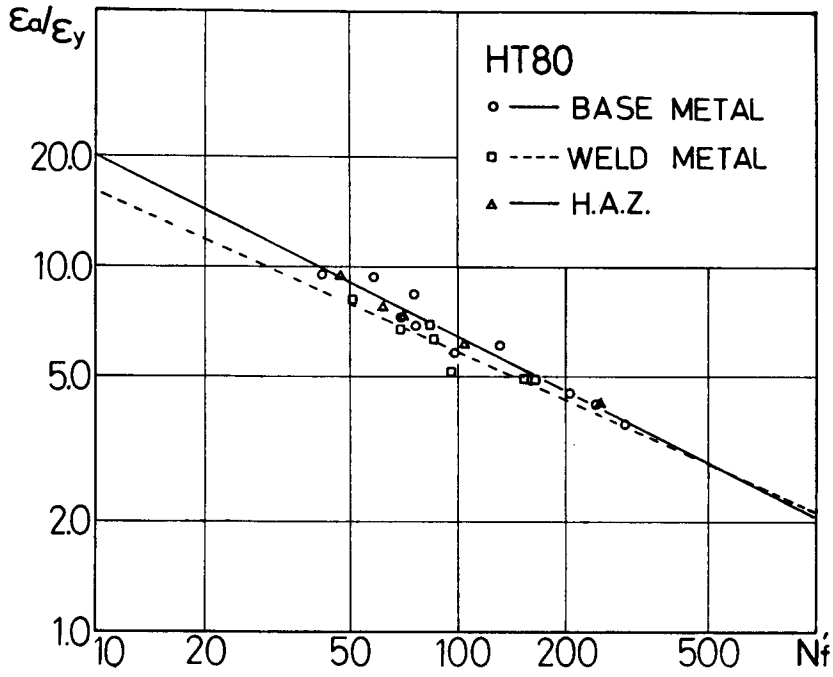

(e)

Fig. 7. The Non-dimensional Strain Amplitudes and the Fatigue Lives

joints. The least squares method was employed for these results, and a linear regression line was obtained for each log-log scale diagram (Fig. 7). A set of approximated relations for every test result is tabulated in Table 6.

Table 6. Linear Regressions with Fatigue Strength

(SS41)	
B.	$\frac{\varepsilon a}{\varepsilon y}=220\cdot(N_f')^{-0.58}+2.6\cdot(N_f')^{-0.10}$
W.	$\frac{\varepsilon a}{\varepsilon y}=240\cdot(N_f')^{-0.63}+3.1\cdot(N_f')^{-0.17}$
H.	$\frac{\varepsilon a}{\varepsilon y}=340\cdot(N_f')^{-0.64}+4.0\cdot(N_f')^{-0.17}$
(SM50B)	
B.	$\frac{\varepsilon a}{\varepsilon y}=160\cdot(N_f')^{-0.57}+2.2\cdot(N_f')^{-0.11}$
W.	$\frac{\varepsilon a}{\varepsilon y}=140\cdot(N_f')^{-0.57}+1.6\cdot(N_f')^{-0.06}$
H.	$\frac{\varepsilon a}{\varepsilon y}=110\cdot(N_f')^{-0.49}+2.0\cdot(N_f')^{-0.09}$
(SM58Q)	
B.	$\frac{\varepsilon a}{\varepsilon y}=99\cdot(N_f')^{-0.57}$
W.	$\frac{\varepsilon a}{\varepsilon y}=42\cdot(N_f')^{-0.39}$
H.	$\frac{\varepsilon a}{\varepsilon y}=48\cdot(N_f')^{-0.42}$
(HT70)	
B.	$\frac{\varepsilon a}{\varepsilon y}=86\cdot(N_f')^{-0.56}$
SW.	$\frac{\varepsilon a}{\varepsilon y}=89\cdot(N_f')^{-0.55}$
CW.	$\frac{\varepsilon a}{\varepsilon y}=69\cdot(N_f')^{-0.50}$
(HT80)	
B.	$\frac{\varepsilon a}{\varepsilon y}=64\cdot(N_f')^{-0.50}$
H.	$\frac{\varepsilon a}{\varepsilon y}=44\cdot(N_f')^{-0.44}$
W.	$\frac{\varepsilon a}{\varepsilon y}=62\cdot(N_f')^{-0.49}$

The quantities of fatigue strength deterioration of these welded joints, if any, could be estimated by using these approximated formulae. As Iida[24] proposed, the fatigue strength ratio (called FSR in this paper) can be obtained for each welded joint as shown in Fig. 8 (a)-(e).

From these figures, the following conclusions can be drawn: For the welded joints of SS41, the deterioration in comparison with the fatigue strength of the base metal was observed in the higher range of fatigue life. On the contrary, for the welded joints of other base metals, it arises at a lower range, except in the case of SM58Q, in which these deteriorations were very slight, that is, about 20% at most. But, the welded joint of SM58Q deteriorates conspicuously at a lower range of cycles, especially at 10 cycles at which point the deterioration reaches approximately 40%.

5. Summary and Conclusions

Using cylindrical specimens for various kinds of base metals and butt-welded joints, this investigation was carried out. With the objective in mind to clarify the cyclic inelastic behaviors and low-cycle fatigue characteristics of welded joints,

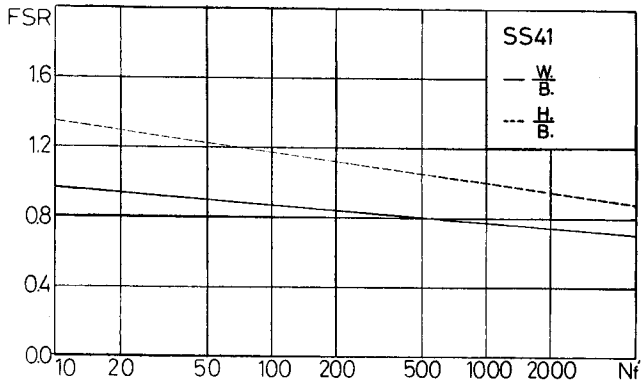
FSR
1.6
1.2
0.8
0.4
0.0
10
20
50
100
200
500
1000
2000
Nf
SS41
W.
B.
H.
B.

(a)

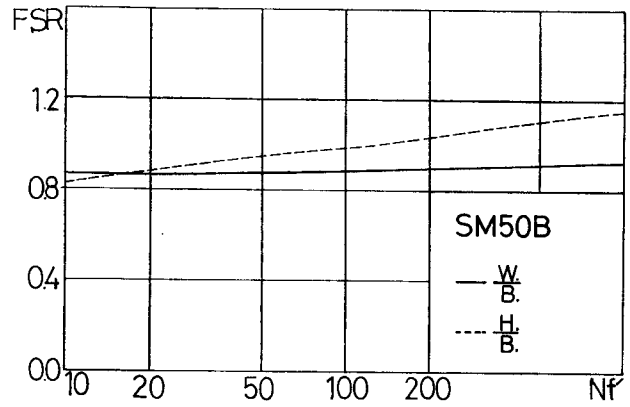
FSR
1.2
0.8
0.4
0.0
10
20
50
100
200
Nf
SM50B
W.
B.
H.
B.

(b)

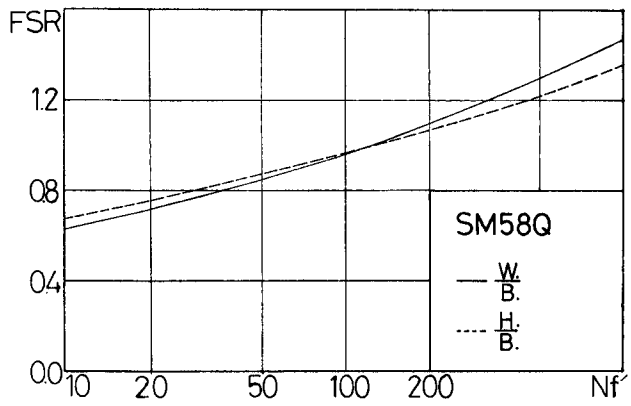
FSR
1.2
0.8
0.4
0.0
10
20
50
100
200
Nf
SM58Q
W.
B.
H.
B.

(c)

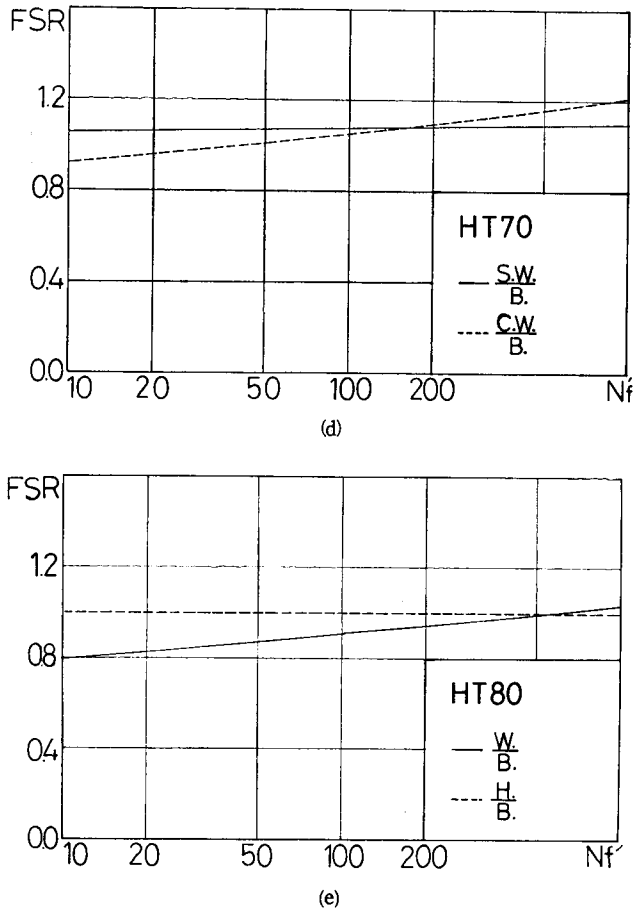

Fig. 8. Fatigue Strength Ratio (FSR) for the Welded Joints

basic to the study of the behavior of beam-column welded joints, which have great influence on the over-all dynamic properties of steel buildings during severe earthquakes.

From the results of this experiment, the following conclusions may be drawn:

[1] The cyclic stress-strain curves which intersect the peak values at the steady-states can be approximately represented by Eqs. (1) and (2).

[2] The non-dimensional plastic strain energy of welded joints, dissipated per cycle at the steady-states, can be formulated by Eq. (3), using the same coefficients as those of specific base metals. These values are shown in Table 5.

[3] The low-cycle fatigue strength for each metal and the welded joint can be estimated by using the specific formulae in Table 6. Low-cycle fatigue deterioration is observed at lower cycles for the welded joints of base metals which

possess higher monotonic tensile strengths. Especially, in the case of the SM58Q welded joint, the fatigue strength ratio is about 60% at 10 cycles. On the other hand, in the case of SS41, a slight deterioration occurs at longer lives. It will be necessary to make a broader and indepth examination of these phenomena which would involved welded joints fabricated by means of other welding procedures, since only a few experiments with respect to the welding procedures have been carried out in this paper.

References

1) S.S. Manson and M.H. Hirschberg; "Fatigue—An Interdisciplinary Approach", p. 133 (1964).
2) J.F. Tavernelli and L.F. Coffin, Jr.; J. Basic Engng. *Dec.*, p. 533 (1962).
3) J.T.P. Yao and W.H. Munse; ASTM *STP***338**, p. 5 (1962).
4) JoDean Morrow; ASTM *STP***378**, p. 45 (1964).
5) G.E. Feltner and JoDean Morrow; J. Basic Engng., *March*, p. 15 (1961).
6) K. Iida; J. Japan Welding Soc., **37**, No. 6, p. 14 (1968).
7) T. Hotta, J. Muraki, T. Ishiguro, N. Ishii and S. Sekiguchi; J. Soc. Naval Architects of Japan, **124**, Dec., p. 341 (1968).
8) T. Hotta, T. Ishiguro, N. Ishii and S. Sekiguchi; J. Soc. Naval Architects of Japan, **126**, Dec., p. 357 (1969).
9) T. Hotta, T. Ishiguro, N. Ishii, K. Miya and S. Sekiguchi; J. Soc. Naval Architects of Japan, **128**, Dec., p. 317 (1970).
10) R.W. Landgraf; ASTM **STP519**, p. 213 (1971).
11) K. Iida and H. Inoue; J. Soc. Naval Architects of Japan, **133**, June, p. 235 (1973).
12) R. Tanabashi, Y. Yokoo, M. Wakabayashi, T. Nakamura, H. Kunieda, H. Matsunaga and T. Kubota; Trans. of A.I.J., **175**, Sept., p. 17 (1970) and R. Tanabashi, Y. Yokoo, T. Kubota and A. Yamamoto; Trans. of A.I.J., **176**, Oct., p. 25 (1970).
13) M. Watanabe and H. Matsuno; J. Soc. Naval Architects of Japan, **131**, June, p. 379 (1972).
14) J. Yagi, Y. Tomita and T. Fukuoka; J. Soc. Naval Architects of Japan, **133**, June, p. 201 (1973).
15) J. Yagi and Y. Tomita; J. Soc. Naval Architects of Japan. **134**, Dec., p. 325 (1973).
16) J. Yagi and Y. Tomita; J. Soc. Naval Architects of Japan, **138**, Dec., p. 410 (1975).
17) I. Kajiraj and J.T.P. Yao; Proc. ASCE, **95**, Aug., p. 1673 (1969).
18) I. Kajiraj; Proc. ASCE, **98**, March, p. 655 (1972).
19) M.T. Suidan and R.A. Eubanks; Proc. ASCE, **99**, May, p. 923 (1973).
20) K. Mizuhata, Y. Gyoten and H. Kitamura; Proc. of Sixth World Conference on Earthquake Engineering, **2**, p. 3031 (1977).
21) J.C. Anderson and R.D. Gupta; Proc. ASCE, **98**, Nov., p. 2523 (1972).
22) R. Tanabashi; J. Japanese Welding Society, **9**, No. 12, p. 587 (1937).
23) E.P. Popov and V.V. Bertero; Proc. ASCE, **99**, June, p. 1189 (1973).
24) K. Iida; Metals in Engineering, **8**, No. 3, p. 11 (1968).
25) T. Naka, B. Kato and H. Aoki; J. of the Japan Welding Society, **37**, No. 12, p. 39 (1968).
26) I. Tatsukawa and A. Oda; J. of the Japan Welding Society, **43**, No. 2, p. 147 (1974).
27) K. Iida, K. Minoda and Y. Kho; J. Soc. Naval Architects of Japan, **144**, p. 371 (1977).
28) K. Kaneta and I. Kohzu; Proc. of the Japan Earthquake Engineering Symposium, p. 1 (1973).